# 20

# Designing one-, two- and three-dimensional left-handed materials

Maria Kafesaki

*Institute of Electronic Structure and Laser (IESL), Foundation for Research and Technology Hellas (FORTH), P.O. Box 1385, 71110 Heraklion, Crete, Greece*

Th. Koschny

*Ames Laboratory and Dept. Physics and Astronomy, Iowa State University, Ames, Iowa 50011, and IESL-FORTH, Crete, Greece*

C. M. Soukoulis

*Ames Laboratory and Dept. Physics and Astronomy, Iowa State University, Ames, Iowa, and IESL-FORTH and Dept.of Materials Science and Technology, University of Crete, Greece*

E. N. Economou

*Institute of Electronic Structure and Laser (IESL), Foundation for Research and Technology Hellas (FORTH), P.O. Box 1385, 71110 Heraklion, Crete, Greece, and Dept.of Physics, University of Crete, Greece*

## 20.1 Introduction

Left-handed materials (LHMs) or negative index materials (NIMs), i.e. materials with simultaneously negative electrical permittivity, $\varepsilon$, and magnetic
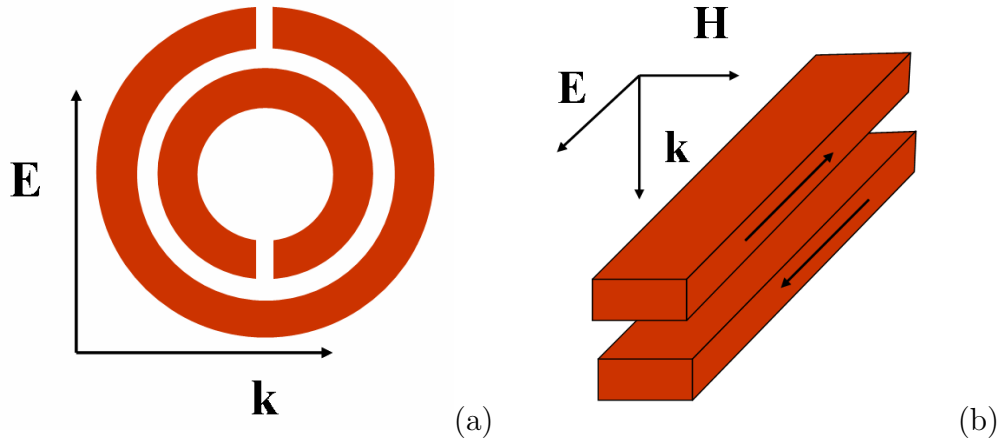
**FIGURE 20.1**  Two of the major designs employed for the achievement of negative permeability response: the SRR, (a), and the pair of slabs, (b). The SRR design of panel (a) is the original design proposed by Pendry et. al. Figure shows also the direction of the incident electromagnetic field which excites the negative permeability response in the designs shown.

permeability, $\mu$, and therefore negative index of refraction, $n$ [*], (over a common frequency range) have received considerable attention over the last years; this is mainly due to their novel and unique properties which provide a huge potential and novel capabilities in the manipulation of electromagnetic waves (for recent reviews see [1, 2]). These properties include backwards propagation (i.e., opposite phase and energy velocities), negative refraction, reversed Doppler effect and Cherenkov radiation, evanescent wave amplification [3] etc., and open new ways in applications like imaging, lithography, antenna systems, transmission lines, various microwave components and devices, etc.

Although many of the the theoretical capabilities of LHMs have been described long ago [4], the first practical implementation of a LHM came only in 2000 [5], by Smith et al., following ideas by Sir J. Pendry et al. [6, 7]; this first left-handed material was a periodic combination of metallic rings with gaps (see Fig. 20.1(a)), known as split-ring resonators (SRRs), providing the negative permeability [7], and continuous wires, providing the negative permittivity [6].

Since Smith's demonstration of the first LHM, several left-handed (LH) structures were demonstrated (see, e.g., [8, 9, 10]), most of them being combinations of SRRs and wires, operating in the microwave regime, and intensive

---

[*]The negative real part of $n$ results by requiring a positive imaginary part, i.e. an attenuated rather than an exponentially growing wave $e^{i(\omega/c)nz}$, where $z$ is the propagation direction.

efforts to understand their behavior, to optimize them (as to achieve a wide left-handed band with high transmittance) and to raise their frequency of operation were carried out. Moreover, alternative ways to achieve left-handed behavior were investigated, such as employing photonic crystals [11], chiral media [12], polaritonic media [13] etc.

Although some of those ways look promising and constitute a subject of intense further investigations, still the most common way to achieve LH behavior is to follow Smith's approach of combining resonant permeability elements (for the achievement of negative permeability response), such as SRRs, with negative permittivity elements, such as thin metallic wires.

The resonant permeability elements are all characterized by the generation of resonant loop-like currents, under the influence of an external alternating magnetic field. These loop currents lead to a resonant magnetic dipole moment, and thus to a resonant permeability in a collection of such "magnetic dipoles", which has the form [7, 2]

$$\mu = \mu_0(1 - \frac{F\omega^2}{\omega^2 - \omega_m^2 + i\omega\gamma_m}). \tag{20.1}$$

In (20.1) $\omega_m$ is the frequency of the magnetic resonance, $\gamma_m$ is a factor representing the losses, and the parameter $F$, determining the strength of the magnetic resonance and the width of the negative permeability regime, is a geometrical factor which is approximately equal to the volume fraction of the loop-current element within the system unit cell. Since the loop-current element is a resonant electromagnetic system, it is very often described as an inductor-capacitor ($LC$) circuit, with the frequency $\omega_m$ given as $\omega_m = 1/\sqrt{LC}$.

The resonant permeability (loop-current) elements which have received most attention up to now are the SRR (of various designs - the original (Pendry's) one is shown in Fig. 20.1(a)) and the slab-pair design [14, 15], i.e. a pair of two parallel slabs (or stripes, or wires), like the one shown in Fig. 20.1(b). This slab-pair is characterized by a resonant current mode with antiparallel currents in the two slabs of the pair, which generate a resonant magnetic moment, making thus the pair to behave like an SRR (it can be seen as a modification of a single-ring SRR with two-gaps). The slab-pair design presents certain advantages compared to the SRR (see Sec. 20.6), especially in small length scale structures aimed to give THz and/or optical LHMs.

Concerning the negative permittivity structures, still the most common one is the periodic system of thin metallic wires. Thin metallic wires behave as a dilute free electron plasma (whose kinetic energy is greatly enhanced by the addition of the magnetic energy), described by a Drude type $\varepsilon$, of the form (in loss-less case)

$$\varepsilon = \varepsilon_0(1 - \frac{\omega_p^2}{\omega^2}). \tag{20.2}$$

$\varepsilon$ in Eq. (20.2) is characterized by a broad negative regime terminated at a reduced plasma frequency [6], $\omega_p$. $\omega_p$ depends on the geometrical system parameters, namely the cross-section of the wires and the periodicity of the medium. For mm scale wires the frequency $f_p = \omega_p/2\pi$ falls in the few GHz regime.

Although there are additional negative permittivity elements that have been proposed in the literature (see, e.g., [16]), in most of them the negative permittivity results from a Lorentz-type permittivity resonance. Thus they are characterized by a narrow negative $\varepsilon$ band and relatively high losses. Therefore, the thin continuous wires still remain the optimum negative permittivity component for the creation of left-handed materials.

Since both SRRs and metallic wires have been described in detail elsewhere in this handbook (see, e.g., Chapters 16 and 18), we will not proceed here to a detailed analysis of their properties; we will comment only on the aspects of their behavior that are essential for their use as components of left-handed materials, which is the central topic of the present Chapter.

Specifically, in this Chapter we discuss some of our efforts to understand the behavior of metamaterials composed of SRRs&wires, slab-pairs, and slab-pairs&wires (in both GHz and optical regimes), and to arrive to conditions for the achievement of optimized left-handed materials, both planar and 2D/3D, employing those structures. The properties of the different media discussed here have been examined and analyzed by transmission ($T$) and reflection ($R$) simulations and/or measurements and, when required, by inversion of the transmission and reflection data to obtain the effective material parameters $\varepsilon$, $\mu$, refractive index, $n$, and impedance, $z = \sqrt{\mu/\varepsilon}$. For the inversion of the $R/T$ data the standard retrieval procedure [17] has been employed, which treats a metamaterial as a homogeneous effective medium.

The Chapter is organized as follows: In Section 20.2 we examine the conditions to achieve LH behavior in combined systems of SRRs and wires; in addition, we present some considerations related with the presence of SRRs asymmetries or with the resonant electric, dipole-like SRR response. We also present there a criterion to unambiguously identify the left-handed regimes in SRRs&wires transmission spectra, which was based on the above considerations. Employing the results of Section 20.2, we examine in Section 20.3 the conditions for the achievement of a homogeneous-like, three-dimensional (3D) left-handed material employing SRRs and wires, and we propose SRR designs appropriate for the achievement of 3D LHMs. We note here that many of the proposed applications of LHMs (especially superlensing applications) require 3D isotropic, homogeneous-like structures.

Since many of the conclusions of our study have been obtained through the retrieval procedure based on the homogeneous effective medium (HEM)

approach, which is fully justified if the characteristic units of the structures are of deep sub-wavelength scale, condition which is not always fulfilled in the SRRs and wires media (and even less in slab-pairs and wires media), we comment on the applicability of this approach in Section 20.4. Specifically, we discuss the artifacts appearing in the form of the HEM-obtained effective $\varepsilon(\omega)$ and $\mu(\omega)$ due to the influence of the periodicity; these artifacts have been analyzed and understood mainly by comparing the HEM results with results of a periodic effective medium approach.

Finally, closing the first part of this chapter, which concerns SRR-based left-handed materials, we discuss in Section 20.5 the possibility to achieve optical SRR-based left-handed materials and the frequency limitations of the left-handed behavior in SRR systems.

One of the most common approaches for obtaining optical left-handed materials is through scaling-down known left-handed microwave designs. SRRs though do not offer an optimized solution in that respect, due to the fact that negative permeability response requires in-plane propagation and thus multi-stack SRR samples. A better solution is offered by the slab-pair design, which exhibits negative permeability response for incidence normal to the plane of the pairs. For that reason, in the second part of this Chapter we discuss slab-pairs and slab-pair-based left-handed materials, mostly in microwaves but also in THz and optical frequencies. In Section 20.6 we discuss the possibility to obtain left-handed behavior using only slab-pairs and exploiting the simultaneous presence of resonant magnetic and resonant electric response in the pair at neighboring frequencies. In Section 20.7 we examine left-handed materials based on slab-pairs and continuous wires, emphasizing the so-called fishnet design, i.e. wide slab-pairs, connected with wires. Finally, in Section 20.8 we discuss the properties of the slab-pair-based designs as the designs are scaled down to give optical left-handed materials.

## 20.2   One-dimensional microwave left-handed materials employing SRRs and wires

Since in a LH material of SRRs&wires the major element for the achievement of negative $\mu$ is the SRR while for the achievement of negative $\varepsilon$ is the wires, the only condition that was sought in the construction of the first and many of the subsequent LHMs was "the negative $\mu$ regime of the SRRs to be within the negative $\varepsilon$ regime of the wires"; thus, the negative $\mu$ and $\varepsilon$ regimes of the SRRs and wires, respectively, have been determined by measuring the transmission properties of the SRRs alone and of the wires alone (the lowest frequency dip in the SRR transmission spectra was considered as originated from a negative $\mu$ response, while the first transition from zero to high transmission in the wires
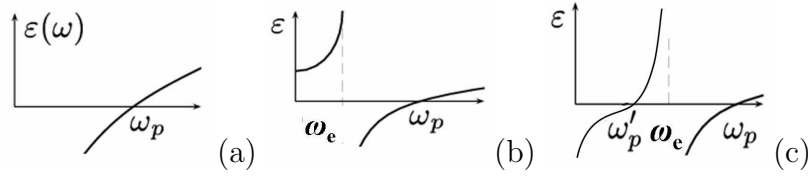
**FIGURE 20.2** Frequency dependence of the effective permittivity, $\varepsilon$, of a system of infinitely long wires, (a), (Drude-type response, characterized by a "plasma-like" frequency $\omega_p = \omega_{p-w}$), and of a system of lossless short wires or SRRs, (b), (Lorentz-type response, characterized by a resonance frequency $\omega_e$ and a "plasma-like" frequency $\omega_p = \omega_{p-SRR}$). In panel (c) the $\varepsilon(\omega)$ resulting from the addition of the $\varepsilon$ of panels (a) and (b) is shown. Note that the new plasma frequency $\omega_p'$ is lower than the wires' plasma frequency, $\omega_{p-w}$.

system was considered as the transition from negative to positive $\varepsilon$ response).

This approach does not provide any safe way to identify unambiguously the presence of negative $\mu$ and, moreover, it neglects any effects coming from the interaction of SRRs and wires or any additional effects that may result from the complexity (e.g. bianisotropy) of the SRR particles [18].

Such effects, which are discussed below, are (a) the influence of the electric dipole-like response of the SRRs on the effective $\varepsilon$ of the SRRs&wires systems, and (b) the effect of the SRR asymmetries on the left-handed behavior of a SRRs&wires medium.

### 20.2.1 Electric response of the SRRs and its role in the electric response of left-handed materials

SRRs are widely studied and used up to now as magnetic elements. Apart from their magnetic response though, they also present a resonant electric-dipole-like response, such as all metallic systems which are finite along the external electric field direction. This resonant electric response, which can be described with a Lorentz-type effective permittivity involving also negative permittivity values, is associated with strong homoparallel currents at the parallel to the external electric field (**E**) sides of the SRR.

In the cases where the magnetic response of the SRR is not in the deep subwavelength regime, like, e.g., in simple SRR designs or multigap SRRs, the electric response frequency of the SRR is not far above its magnetic resonance frequency, and contributes to the low frequency electric response of the combined system of SRRs&wires. Detailed studies of this contribution [19] have shown that the total effective $\varepsilon$ of a SRRs&wires medium is the one resulting from the addition of a Drude-like $\varepsilon$ response (coming from the wires - see Fig. 20.2(a)) with the a Lorentz-like $\varepsilon$ response (coming from the SRRs - see Fig. 20.2(b)), and has the form shown in Fig. 20.2(c).
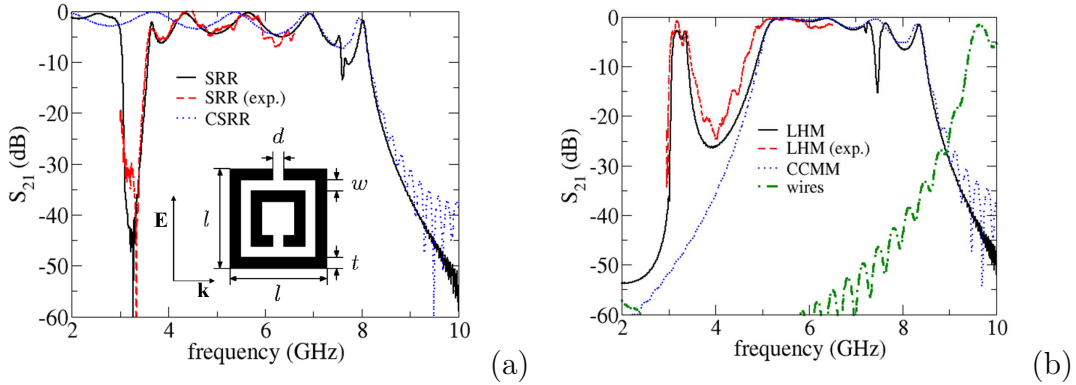
**FIGURE 20.3**    (a): Simulated (solid line) and measured (dashed line) transmission amplitude ($S_{21}$) of a 5-unit cells (uc) periodic arrangement of square SRRs. The dotted line shows the simulated $S_{21}$ after closing the gaps of the SRRs. Notice that by closing the SRR gaps the dip at ∼3 GHz disappears while the rest of the spectrum remains unaffected. This indicates that the ∼ 3 GHz dip is magnetic in origin, while the dip after 8 GHz is due to negative $\varepsilon$ behavior. (b): Simulated (solid line) and measured (dashed line) transmission ($S_{21}$) spectra of a left-handed material composed of SRRs (like the ones described in panel (a)) and wires, in a periodic arrangement (5 uc). The dotted line shows the $S_{21}$ of the combined material of closed-SRRs and wires (CCMM) and the dotted-dashed line the $S_{21}$ for the wires only. Notice that the plasma frequency of the CCMM (at ∼5 GHz) is much lower that the plasma frequency of wires only, which is at ∼9 GHz. Notice also that the only difference between the transmission of LHM and CCMM is the left-handed peak at ∼3 GHz, showing that the CCMM carries all the electric response of the LHM. The geometrical parameters of the system are: uc size $8.8 \times 8.8 \times 6.5$ mm$^3$, $l = 7$ mm, $d = w =$0.2 mm, $t = 0.9$ mm (see inset), metal depth = 30 $\mu$m, wires width=0.9 mm. The SRRs and wires are printed on opposite sides of a PCB board of thickness 1.6 mm and $\varepsilon = 2.8$. The wires are placed symmetrically to the SRRs, along the imaginary line connecting the two SRR gaps. (Figure From Ref. [21].)

The result of this addition which is more relevant for the construction of a LHM is a downwards shift of the effective plasma frequency of the system, $\omega'_p$, compared to that of only the wires, $\omega_p$. This shift poses stringent requirements for the achievement of LH behavior: for a SRRs&wires medium to be left-handed the magnetic SRR resonance frequency, $\omega_m$, should lie not only below $\omega_p$, but also below the new cut-off frequency, $\omega'_p$. (Note that if $\omega_p < \omega_m < \omega'_p$, a case very common in practical implementations, ignoring the SRR electric response and its effect may result to a wrong identification of the character of the transmission peaks [20].)

Another observation of large practical importance is the following: By closing the gap/gaps of the SRR its magnetic response is switched off (since the resonance of the loop-like currents is destroyed), but the electric SRR response is entirely preserved [19, 21, 2] (this is valid though only for SRRs with mirror symmetry with respect to the external electric field). Therefore, the closing

of the SRR gaps can led to the identification of both the negative $\mu$ and the negative $\varepsilon$ regimes of a SRRs system, as is shown in Fig. 20.3(a), and also of a SRRs&wires system, as is shown in Fig. 20.3(b), offering hence an easy way to unambiguously identify the left-handed regimes. This way is extremely valuable in experimental studies, as it provides an easy to apply criterion to unambiguously conclude if a structure is left-handed or not.

### 20.2.2 Bianisotropy of SRR and its influence on the LH behavior

Investigating the effect of the SRR orientation on the left-handed behavior of a SRRs&wires system, for various SRR types [22, 23], we found that another aspect of the electromagnetic response of the SRR which is crucial for its ability to create LHMs comes from its bianisotropy [18, 24], which gives the possibility of excitation of its magnetic resonance (i.e. the resonant oscillation of the circular currents around its rings) by the external electric field, **E**. This Electric field induced Excitation of the Magnetic Resonance (EEMR effect) occurs whenever the SRR does not present mirror symmetry with respect to **E**, as is shown and explained in Fig. 20.4(b); it occurs even for incidence normal to the SRR plane [22]. One result, among others, of the resonant circular currents excited in the asymmetric SRR is the non-zero average polarization induced, which is translated to a resonant permittivity response (in a homogeneous effective medium description) at the magnetic resonance frequency [22, 21, 23].

A resonant permittivity response at the magnetic resonance frequency can be detrimental for the achievement of LH behavior in SRRs&wires systems, as it imposes strong positive $\varepsilon$ regimes where negative $\varepsilon$ is required. The effect is even more detrimental in two-dimensional (2D) and three-dimensional (3D) SRRs&wires systems designed to create LHMs, where one requires that the SRRs which do not contribute to the magnetic response of the medium to be also electrically inactive. In such systems, especially in 3D, EEMR can be avoided only by employing symmetric SRR designs, like, e.g., multigap SRRs [23]. (Note that in 1D or even 2D systems the effect can be avoided by orienting properly the SRRs.)

Despite the detrimental influence of the EEMR effect on the achievement of LH behavior in SRRs&wires systems, this effect presents an important advantage in the study of small (micrometer and nm scale) SRR systems, since it offers an indirect way to trace the SRR magnetic resonance regime in transmission experiments, i.e., by using normal incidence in one or few SRR layers. This advantage has been exploited very extensively recently, as it was used to demonstrate experimentally the occurrence of a magnetic SRR resonance in the 6 THz [25], 100 THz [26] and 1.5 mm [27] regimes.
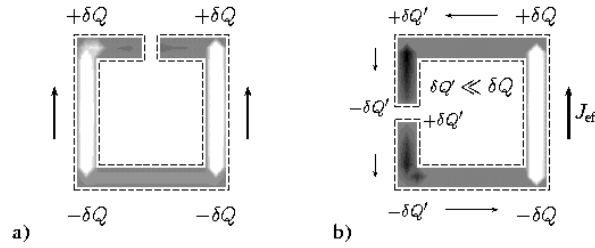
**FIGURE 20.4**    Simple drawing for the charge and current for a symmetric, (a), and a non-symmetric, (b), single-ring SRR in an external electric field, $\mathbf{E}$ (pointing upwards). The interior of the ring shows simulation data for the polarization current component $J||E$ at a fixed time for normal incidence; white color indicates upwards current and black downwards current. The asymmetry of the SRR in the case of panel (b) leads to different electric field induced charges at the two top and bottom corners of the SRR and thus to a potential difference which is compensated by a circular current. (Figure from Ref. [22].)

## 20.3    2D and 3D left-handed materials from SRRs and wires

Since many of the proposed applications of LHMs, such as the superlensing based applications, require 2D or 3D isotropic, homogeneous-like materials, many attempts have been made to realize such metamaterials (see, e.g., [28, 29, 30, 31, 32, 33]). Besides the practical problems though in such a realization, there are many fundamental considerations that should be taken into account for the achievement of a 3D homogenous-like and isotropic LHM using SRRs and wires.

One impeding factor, which was discussed in the previous section, is the presence of the SRR's asymmetries, which produces electric resonances (resonances in $\varepsilon$) at the magnetic resonance frequency regimes, destroying the negative $\varepsilon$ response required for the achievement of left-handed behavior. Therefore, for the achievement of 2D and mainly 3D left-handed materials it is essential to employ fully symmetric SRR structures. An example of such a structure is a symmetric 4-gap SRR, as the one shown in Fig. 20.5(a) [31]. The presence of many gaps though, as in the design of Fig. 20.5(a), leads to an upwards shift of the magnetic resonance frequency [32, 23] (gaps act like capacitors in series, reducing the total capacitance of the structure, and increasing thus the magnetic resonance frequency, $\omega_m = 1/\sqrt{LC}$); as a result, it is difficult for the magnetic resonance frequency to fall in the negative $\varepsilon$ regime of the system, while it may be pushed close to the periodicity-induced band-gaps; hence, design modifications are essential in this structure. Such modifications can be achieved through the introduction of a high index material in the SRR gaps (as in the case of Fig. 20.5(a)) [31], or through the introduction of proper extensions in the gaps [23], as to increase the gap capacitance (e.g. overleaf capacitors, extra branches - see Fig. 20.5(c) -, etc.), or by using, instead of
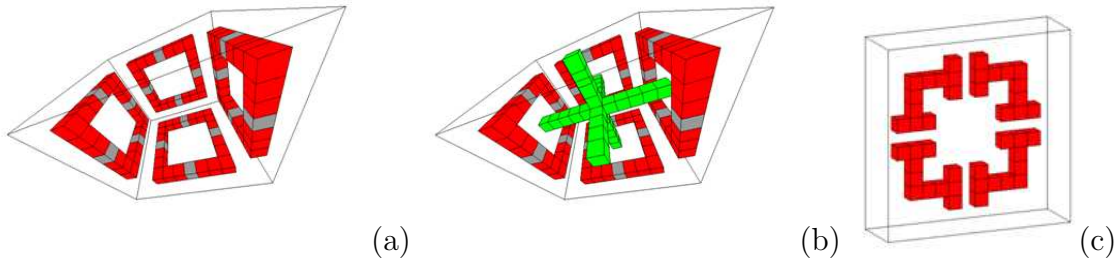
**FIGURE 20.5**  The design of a fully symmetric unit-cell for a one unit-cell-thick slab of an isotropic 4-gap SRR, (a), and a LHM, (b). The interfaces are parallel to the left and right SRR. The SRR gaps are filled with a material of high dielectric constant (light-gray) to reduce the magnetic resonance frequency. An alternative way to reduce the magnetic resonance frequency is to design extensions in the SRR gaps, (c), which increase the gap capacitance. (Figure from Ref. [31].)

single rings, ring-pairs with broad-side (face to face) coupling.

Apart of the requirement of symmetric and of subwavelength scale SRR structures though, there are additional conditions required for the material to approach the isotropic homogeneous effective medium behavior. Such conditions, which are described in detail in Ref. [31], are the inversion symmetry of the unit cell along propagation direction, the inversion symmetry in at least one of the two directions perpendicular to that of the propagation (to avoid cross-polarization effects), and a proper choice of the relative position of SRRs and wires as to minimize the cross-talk between them; such optimum position was found to be the one of Fig. 20.5(b), with the wires aligned in the middle of the SRRs.

## 20.4   Effects of periodicity in the homogeneous effective medium retrieved parameters in SRRs and wires metamaterials

Most proposals for applications based on the unique physical properties of LHMs rely on the homogeneity of the material, in addition to specific values and dispersion of the metamaterial's impedance and refractive index. For instance, a perfect lens, even with exact parameters $n = -1$ and $z = 1$, will only amplify evanescent wave components with momenta smaller than the inverse unit cell size of the LHM [34]. Similar restrictions apply to all super resolution imaging and even cloaking applications of metamaterials.

Homogeneous-like effective medium behavior occurs in metamaterials when the structural length scale of the material becomes much smaller than the wavelength of the electromagnetic radiation propagating through it. Under this condition the metamaterial will behave like a homogeneous medium characterized by just two (in the absence of magnetoelectric coupling) frequency

dependent parameters: the effective permeability, $\mu(\omega)$, and the effective permittivity, $\varepsilon(\omega)$. (Both of them may be tensors if the material is anisotropic.)

One of the key benefits of metamaterials is that we have - in principle - full control over both their magnetic and electric response, such that achieving a LHM with large wavelength to unit cell size ratio becomes possible (current state of the art is about 70 to 200 for microwave metamaterials).

If homogenization of a metamaterial, i.e. the description as an effective homogeneous medium, is possible, we expect the effective parameters $\mu(\omega)$ and $\varepsilon(\omega)$ to be only functions of the frequency, and not of the wave vector. The effective parameters then can be derived by a simple retrieval procedure [17, 35], essentially equating the plain wave scattering amplitudes of a metamaterial slab with those of a finite homogeneous slab of same thickness, and solving for the $\mu(\omega)$ and $\varepsilon(\omega)$, or, equivalently, refractive index, $n(\omega)$, and impedance, $z(\omega)$, of the slab. If these parameters can be chosen independent of the length of the metamaterial, they constitute effective homogeneous medium parameters describing the scattering properties and the propagation inside the metamaterial.

Early microwave metamaterials and all recent metamaterials in the THz and optical regime suffer from the difficulty to reduce the structural size to vacuum wavelength ratio beyond the range of 5 to 10, while maintaining reasonable response amplitudes and losses. In this region, the effective parameters retrieved for the metamaterials show strong artifacts [36] that were not expected from the simple analytic theory. They indicate the beginning of the breakdown of the homogeneous medium behavior and the transition into a multiple scattering dominated regime, as in a photonic crystal. These artifacts include: (i) the resonant index of refraction is cut-off close to the resonance, at values for which the wave vector inside the material approaches the Brillouin zone edge; (ii) the discontinuities marking the position of the resonance as retrieved from the effective refractive index and impedance (or $\varepsilon$ and $\mu$) do not coincide but are shifted in frequency; (iii) the expected Lorentzian shape of the magnetic resonance is strongly deformed, usually with the positive part cut-off; (iv) an unexpected anti-resonant behavior in $\varepsilon(\omega)$ is found whenever $\mu(\omega)$ is resonant, and vice versa; (v) seemingly unphysical negative imaginary parts occur in the effective medium parameters $\mu(\omega)$ and $\varepsilon(\omega)$.

All those artifacts can be understood and quantitatively predicted taking the inherent periodicity of the metamaterial into account [37]. In the long wavelength limit all of these artifacts vanish (except in very close proximity to a strong, low-loss resonance) and the expected behavior of a Lorentz-like resonant $\mu(\omega)$ and a smooth plasmonic $\varepsilon(\omega)$ are recovered. For a typical microwave SRR&wire LHM this would require a wavelength to unit cell ratio of the order of 50.
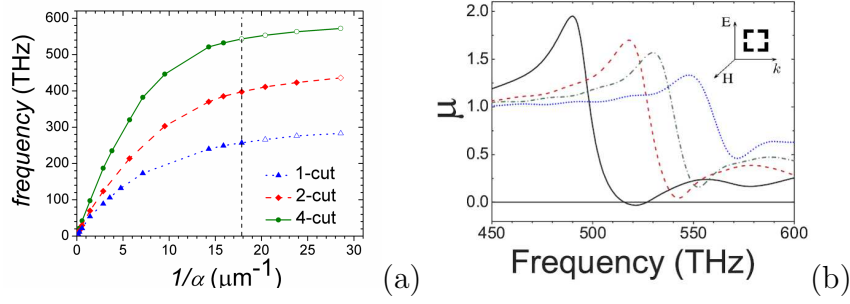
**FIGURE 20.6**    (a): The scaling of the simulated magnetic resonance frequency, $f_m = \omega_m/2\pi$, as a function of the linear size, $a$, of the SRR unit cell, for single-ring SRRs of one, two and four gaps (cuts). Up to lower THz region the scaling is linear. The maximum attainable frequency is strongly increased with the number of gaps in the SRR ring. The hollow symbols and the vertical line at $1/a$=17.9 $\mu m^{-1}$ indicate that no negative $\mu$ is reached beyond this value. For the SRR designs employed the unit cell has dimensions $a \times a$ in the SRRs plane and $0.614a$ perpendicular to it. The SRR is made of Aluminum, simulated with a Drude-type permittivity. (b): Simulated Re $\mu$ for a single-ring 4-gap SRRs system, for unit cell sizes $a = 70$ nm (solid line), 56 nm (dashed line), 49 nm (dotted-dashed line) and 35 nm (dotted line). (Figure from Ref. [39].)

These periodicity artifacts are usually strongly detrimental to the desired metamaterial properties and their avoidance constitutes an additional constraint for metamaterials design. Further, also the symmetry of the unit cell and the metamaterial sample places some constraints on the effective medium behavior [35] (see previous section), which need to be accounted for in LHMs design.

## 20.5    SRRs and wires metamaterials towards optical regime

The novel and unique properties of LHMs, which result to new capabilities in the manipulation of EM waves, have as a result a strong effort worldwide to achieve such materials not only in the microwaves, where they were initially demonstrated, but also in the THz and optical regimes [38], targeting applications such as imaging, security, sensing, lithography, etc.

One of the most straightforward approaches to achieve THz and optical LHMs is the scaling of established microwave LH structures, like the SRRs&wires structures. Since though the properties of the metal, which is the main constituent of most to date's metamaterials, are drastically different in the optical regime compared to those in the microwaves (there, the metal practically behaves as a perfect conductor), scaling of the structures is not expected to produce always proportional scaling of the resulting properties; thus a detailed examination of the scaling behavior of both SRRs and wires is essential.

Such an examination of the scaling properties of the SRRs [39, 40] revealed

that by scaling the structures the magnetic resonance frequency, which in microwaves scaled inversely proportional to the structure size, close to the optical regime saturates to a constant value (see Fig. 20.6(a)), which depends mainly on the SRR design (geometrical characteristics). Moreover, the magnetic permeability resonance becomes weaker and weaker as we approach the sub-micron scale, and after some length-scale it ceases to reach negative values (see Fig. 20.6(b)). Both of these effects can be explained by taking into account the kinetic energy of the current-carrying electrons inside the SRR rings, besides the magnetic energy produced by those current-carrying electrons. This kinetic energy, which in microwaves is negligible compared to the magnetic energy and is usually ignored, in higher frequencies becomes more and more important, mainly due to the large reduction of the magnetic energy as the SRR becomes smaller and smaller.

Considering the electrons kinetic energy through an equivalent inductance, $L_e$, (added to the magnetic field inductance, $L$) in an $LC$ circuit description of the SRR [39, 40, 41], and examining the scaling behavior of $L_e$ (resulting to be $\propto 1/size$), $L$ ($\propto size$) and $C$ ($\propto size$), one obtains for the magnetic resonance frequency the form

$$\omega_m = \frac{1}{\sqrt{(L + L_e)C}} \propto \frac{1}{\sqrt{size^2 + const.}}, \qquad (20.3)$$

which leads to a constant value as the SRR size tends to zero.

Accurate numerical simulations employing practically achievable SRRs [39, 40, 43] have demonstrated this saturation behavior and have shown negative permeability up to 500 THz (600 nm) (in 4-gap SRRs - see Fig. 20.6(b)), i.e. the visible range, indicating the possibility to achieve LHMs even in the visible, by employing SRRs.

If one takes into account also the potential energy of electrons inside the SRR [42], it can be concluded that the theoretical absolute upper limit for the magnetic resonance frequency (assuming the "optimum" SRR design) is the plasma frequency of the bulk metal. In practical cases though, the upper limit that can be achieved is much below that frequency. We have to mention finally that the saturation of the magnetic resonance frequency in nm-scale SRRs has been also demonstrated experimentally [43], for a single-ring, single-gap SRR system.

## 20.6   Slab-pairs and slab-pair-based left-handed materials

Although the SRRs&wires geometry proposed by Pendry has become very widely used in the microwaves regime, this topology presents certain disadvantages in the THz and optical regime requiring micron and submicron

length-scale structures. Its major disadvantage comes form the fact that the negative permeability SRR response is achieved for propagation parallel to the SRR plane (as to have magnetic field perpendicular to that plane), which makes essential the fabrication of multilayer samples, somehow difficult to be achieved with the current technological limitations.

An alternative design which overcomes the above impediment is the slab-pair design (see Fig. 20.1(b)), which was proposed by the Purdue group in 2002 [14]. As it can be concluded from Fig. 20.1(b), the slab-pair design responds as a resonant magnetic dipole for propagation normal to the plane of the structure, which makes possible the demonstration of negative permeability response with a single or very few structure layers. Moreover, the design is very simple and relatively easy to be fabricated in the micro- and nano-scale.

Besides the resonant magnetic mode associated with resonant antiparallel currents at the two slabs of the pair, the slab-pair design allows also a resonant electric mode, associated with parallel currents at the slabs, resulting to a resonant electric dipole moment. Therefore, besides the resonant and negative permeability response, there is also a strong resonant (and with negative values) permittivity response in slab-pair systems, which can occur in frequencies close to the magnetic resonance frequency.

The simultaneous existence of negative $\varepsilon$ and $\mu$ at nearby frequencies in slab-pair systems has led to many attempts to achieve left-handed behavior employing only slab-pairs [15] and tuning properly the negative $\mu$ regime as to fall within the negative $\varepsilon$ regime (which is much broader, due to the stronger electric resonance [44]).

Detailed theoretical studies though [44] have shown that such a "coincidence" can be achieved only under very extreme conditions, while it is impossible for isolated pairs (where the magnetic resonance frequency is always below the electric resonance one). The factor that makes a "coincidence" possible in a periodic system of pairs is the capacitive interaction of neighboring pairs along the electric field direction, which can lead to a large downwards shift of the electric resonance, bringing it below the magnetic one. Modifications of the slab-pair design as to increase this interaction give additional possibilities for the achievement of left-handed behavior using only slab-pairs. Such design modifications (T-type extensions) have been exploited recently for the demonstration of left-handed behavior in slab-pairs at the GHz regime [45].

The difficulty to achieve electric and magnetic resonances at nearby frequencies in only slab-pair systems is based to a large degree on the fact that both the electric and the magnetic resonances result from the splitting of a "single particle dipole resonance" (single-slab resonance), due to the interaction of the slabs of the pair. This is confirmed further by the fact that the dominant pa-
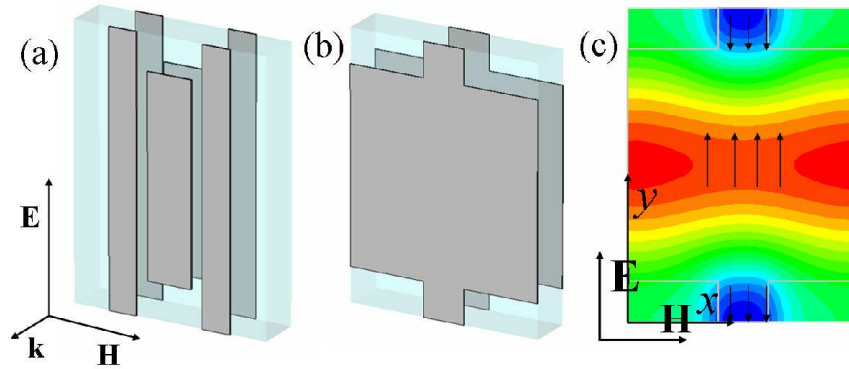
**FIGURE 20.7**    (a): The unit cell of a left-handed metamaterial design based on combination of slab-pairs and continuous wires. Picture shows also the orientation of the external electromagnetic (EM) field that excites the left-handed response of the structure. (b) One unit cell of the fishnet design. The external EM field for the excitation of the LH behavior of the design is as shown in panel (a). (c): The magnetic field component $H_x$ at the magnetic resonance frequency of the fishnet design. The field is plotted at the $x - y$ (or **H**-**E**) plane which lies in the middle (along $z$ direction) of the two metallic sheets of the structure. Dark color indicates large field amplitude and light color low amplitude. (Figure from Ref. [49].)

rameter determining both resonance frequencies (in GHz slabs) is the length of the slabs. The magnetic resonance frequency, in particular, seems to be almost independent of all the other geometrical parameters, i.e. slab-width, thickness of metal and separation of the slabs [44]. (This result that can be easily explained through a *LC* description of the system.)

Closing this section, we have to mention that the achievement of LH behavior only from slab-pairs, besides the disadvantage of being possible only under very extreme conditions, has the additional disadvantage that it stems from the involvement of two resonances, which is associated with large induced looses.

## 20.7    Left-handed behavior from slab-pairs and wires - The fishnet design

Another approach for the achievement of LH behavior that seems to overcome the above mentioned disadvantages of the slab-pair-only LHMs is to combine the slab-pairs with continuous wires, as is shown, e.g., in Fig. 20.7(a), utilizing only the resonant magnetic response of the pairs and making use of the broad negative $\varepsilon$ regime offered by the wires. This approach has been exploited recently for the demonstration of left-handed behavior in both the GHz and the THz regimes [46, 47, 48].

Despite the fact that the addition of wires offers an easier and safer approach compared to the only-slabs one, certain considerations should be taken into

account also here, stemming mainly from the presence of the electric resonance of the slabs at frequencies close to that of the magnetic resonance. As it is described in Section 20.2 for SRRs&wires, also in slabs&wires systems the electric response of the slabs modifies the effective permittivity of the system (compared to that of only the wires), leading to a new plasma frequency, $\omega_p'$, below that of the wires and below the electric resonance frequency of the slabs, $\omega_e$. The influence of the slab's electric resonance though, besides the dramatic in some cases lowering of the plasma frequency, results also to a very abrupt $\varepsilon$ dispersion close to the new plasma frequency. This comprises a serious impediment for the achievement of a good impedance match of the structure with its environment and thus for the achievement of left-handed behavior with high transmittance.

Studying in detail the dependence of the characteristic frequencies of the system on the various system parameters [44], it can be seen that to ensure negative $\mu$ regime below the new plasma frequency $\omega_p'$, one needs relative isolated slabs (i.e. short slabs compared to the corresponding unit cell side), as to ensure magnetic resonance below the electric one.

Moreover, to minimize the destructive influence of the electric resonance on the system's impedance one needs to push the electric resonance not just above the magnetic one but at frequencies as further up as possible. Examining the dependence of the electric resonance frequency on the various system parameters it was found [49] that a large upwards shift of the electric resonance without affecting much the magnetic resonance frequency can be achieved by widening the slabs, reducing thus their inductance. (This widening, despite the fact that it does not affect the magnetic resonance frequency, has a positive influence on the magnetic resonance strength, reinforcing it - due to the increase of the volume available for the induced magnetic field.)

Another factor that leads to upwards shift of $\omega_e$ is to physically connect the slabs with the wires, as is shown in Fig. 20.7(b), which results to a design known as fishnet [50, 51, 49]. Fishnet design, which is described below, seems to offer an optimized solution for the achievement of left-handed behavior, both in microwaves [49] and optical regime [52, 53].

### 20.7.1 The fishnet design

The fishnet design [50, 51, 49], shown in Fig. 20.7(b), combines strong magnetic response and high enough electric ($\varepsilon$) resonance frequency, due to the wide slabs and the physical connection of slabs and wires.

Detailed numerical simulations [49] and corresponding experiments for the fishnet design in the GHz regime [54, 55] have shown left-handed behavior with high transmittance for a wide range of geometrical parameters, making it an

optimized design for the achievement of left-handed behavior. The superior performance of the design has been revealed also in the optical regime, where fishnet has given the highest in frequency [53] and the highest in transmittance levels [52] left-handed materials up to now.

Responsible for this superior performance of the fishnet seem to be the strong magnetic response (as a result of the wide slabs), combined with the smooth, Drude-like electric response (as a result of the high electric resonance frequency) [49]. This smooth electric response results to a good impedance match with the environment for a wide range of geometrical parameters of the structure, and thus to high left-handed transmittance (if the material losses are also low).

The high electric resonance frequency together with all the other characteristics of the structure behavior can be understood through examination of the current and the electric and magnetic field at the resonances of the structure. Such an examination has revealed strong inductive response not only at the slabs of the pair but also at the joints connecting the neighboring slabs along the external **E** direction (see Fig. 20.7(c)). This response, taken into account through an equivalent inductance, parallel to the slabs inductance, can account for all the aspects of the behavior of the structure. Taking into account the joint's inductance and employing simple analytic formulas for the capacitances and inductances of the structure, one can reproduce and explain the dependence of both the magnetic and electric resonance frequency from all the geometrical and material parameters of the fishnet design [49].

Another worth-mentioning characteristic of the fishnet is the slightly higher magnetic resonance frequency compared to the magnetic resonance frequency of only the slabs. This feature, which can be also explained through the joints' loop inductance, although it is not desired in the GHz regime (as it makes the structure less subwavelengh in scale), it is highly desired in the optical regime, as we discuss below.

## 20.8   Slab-pair-based systems towards optical regime

As it has been mentioned in Section 20.5, where we discussed the scaling behavior of SRRs, the non scalability of the metal parameters as one goes from microwaves to the optical regime results to non-scalability of the properties of the artificial magnetic and of the left-handed structures.

This non-scalability observed in the SRRs is repeated (as is expected) also for the structures based on slab-pairs [42, 56], including the fishnet design.

Fig. 20.8(a) shows the magnetic and the electric resonance frequency for a pair of relatively narrow slabs (as the ones of Fig. 20.7(a) - without the wires) and Fig. 20.8(b) the same frequencies, with the addition of the plasma
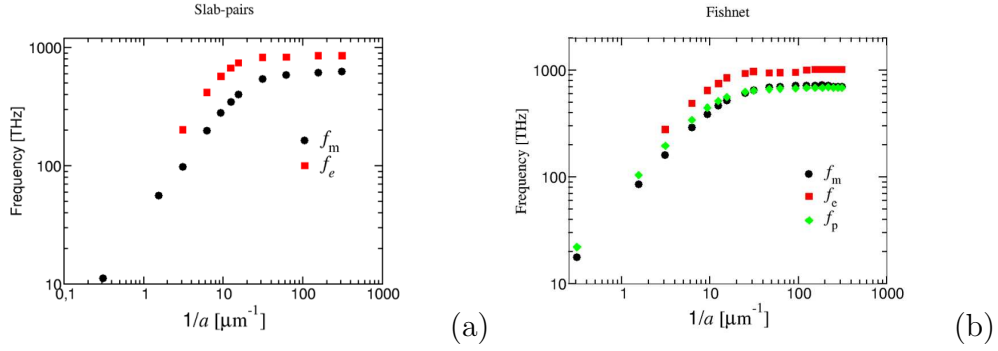
**FIGURE 20.8** The scaling of the simulated magnetic resonance frequency, $f_m = \omega_m/2\pi$, and the electric resonance frequency, $f_e = \omega_e/2\pi$, as a function of the inverse unit cell size, $a$, ($a$ here is the unit cell side along propagation direction) for a system of slab-pairs (panel (a)) and for a fishnet structure (panel (b) - for the design see Fig. 20.7(b)). Panel (b), in addition, shows the scaling of the "plasma" frequency, $f_p = \omega'_p/2\pi$ (i.e. the frequency of the first transition from negative to positive real part of the structure permittivity), for the fishnet design. The structures have been simulated using the Drude model for the permittivity of the metallic components, with the Aluminum parameters for the plasma frequency (3570 THz) and the collision frequency (19.4 THz), while the dielectric spacer between the metallic elements has been chosen to be glass, with permittivity 2.8. The unit cell parameters are: $2.97a \times 2.19a \times a$, along the external $\mathbf{E}$, $\mathbf{H}$ and $\mathbf{k}$ direction respectively (for the designs and axes see Fig. 20.7), the slabs thickness is $0.25a$, the width (along $\mathbf{H}$) of the joints is $0.47a$, the board thickness (along $\mathbf{k}$) is $0.5a$, the slabs length $2.19a$ and the narrow-slabs width is $0.47a$. (Figure from Ref. [56].)

frequency, $f_p = \omega'_p/2\pi$, for the fishnet design. Both results show the saturation of all the characteristic metamaterial frequencies. Calculations of the magnetic permeability close to the saturation regime show also here the weakening of the permeability resonance going to higher and higher frequencies [56].

Both the saturation of the magnetic and the electric resonance frequencies, as well as the weakening of the resonance strength can be explained, like for SRRs, through the "kinetic inductance" of the electrons inside the metal. (Note that the involvement of the kinetic inductance results to involvement of additional geometrical parameters in the determination of the magnetic resonance frequency, which in the GHz range was found to be determined almost exclusively by the length of the slabs.)

Comparing the saturation values of the magnetic resonance frequency of the pairs with those of single-ring single-gap SRRs, one can observe higher saturation values for the pairs. This is due to the decreased capacitance (because of the two gaps) and inductance (because of the reduced area) of the pair compared to single-ring, single-gap SRR.

From Figs. 20.8 it is worth-mentioning also that: (a) Fishnet maintains the observed in microwaves higher magnetic resonance frequency - compared to only slab-pairs - also close to the saturation regime. (b) Electric resonance frequency, both for slab-pairs and fishnet, maintains its higher values compared to magnetic resonance frequency in all frequency ranges, including the saturation regime. (c) The plasma frequency for the fishnet, $f_p$, although it is higher than the magnetic resonance frequency in the microwaves, it does not maintain its higher values in the saturation regime; thus design modifications are required for the structure to maintain its left-handed behavior as it is scaled down. This shows that an optimized left-handed microwave design is not necessarily the preferred left-handed design at the optical regime.

Finally, we have to mention that consideration of the kinetic inductance of the slab electrons can explain all the above features and can give simple approximate analytical formulas for the various saturation values [56], which can be very useful for structure optimizations.

An overall structure optimization, though, should take into account not only the effects associated with the kinetic inductance, but also the other important factor for the achievement of functional optical left-handed materials: the minimizations of the resistive losses, unavoidable in such materials. Proposed solutions for such a minimization include changes in designs [57] and optimization of the quality of the constituent materials (e.g., using silver for the metallic components), but also incorporation of gain media into left-handed materials, to compensate for the losses [58]. This last solution is studied extensively recently and might constitute one of the most promising ways for achievement of functional optical left-handed materials.

## 20.9   Conclusions

The unique properties and capabilities of left-handed materials have led to a widespread recognition of them and to exponentially increasing research efforts devoted to their study and exploitation. In this chapter, we attempted a summary of basic design considerations aiming at the achievement of optimized left-handed materials in one- two- and three- dimensions, and in frequency regimes ranged from microwaves to optics.

This kind of structures will be capable to fully demonstrate all the unique properties and abilities of left-handed materials, such as (a) the ability to match the vacuum impedance, which is a unique property of LHMs with many applications (e.g., in stealth technology), (b) the possibility for coupling with the magnetic component of an electromagnetic field without the presence of any magnetic material (this is a new capability of fundamental importance, especially in the terahertz region where no natural magnetic materials exist), (c) the possibility to miniaturize devices and components such as antennas and waveguide structures, leading to very important potential system weight and size savings, and (d) the negative refraction and the subwavelength resolution capability, which open up the possibility of new applications in optics and communications.

## References

[1] D.R. Smith, J.B. Pendry & M. Wiltshire, "Metamaterials and negative refractive Index", *Science* **305**, 788 (2004).

[2] C. M. Soukoulis, et al., "Negative index materials: New frontiers in optics", *Adv. Mat.* **18**, 1941 (2006);

[3] J. B. Pendry, "Negative refraction makes a perfect lens", *Phys. Rev. Lett.* **85**, 3966 (2000).

[4] V. G. Veselago, "The electrodynamics of substances with simulatenous negative values of $\varepsilon$ and $\mu$", Sov. Phys. Usp. **10**, 509 (1968) [Usp. Fiz. Nauk **92**, 517 (1967)].

[5] D. R. Smith et al, "Composite medium with simultaneously negative permeability and permittivity", *Phys. Rev. Lett.* **84**, 4184 (2000).

[6] J. B. Pendry, A. T. Holden, W.J. Stewart and I. Youngs, "Extremely low frequency plasmons in metallic mesostructures", *Phys. Rev. Lett.* **25**, 4773 (1996); J. B. Pendry, A. J. Holden, D. J. Robbins, and W. J. Stewart, "Low frequency plasmons in thin wire structures", *J. Phys. Cond. Matt.* **10**, 4785 (1998).

[7] J. B. Pendry et al., "Magnetism from conductors and enhanced non-linear phenomena", *IEEE Trans. MIT* **47**, 2075 (1999).

[8] R. A. Shelby, D. R. Smith & S. Schultz, "Experimental verification of a negative index of refraction", *Science* **292**, 77 (2001).

[9] C. G. Parazzoli et al., "Experimental verification and simulation of negative index of refraction using Snell's law", *Phys. Rev. Lett.* **90**, 107401 (2003); K. Li et al., "Free-space focused-beam characterization of left-handed materials", *Appl. Phys. Lett.* **82**, 2535 (2003).

[10] M. Bayindir, et al., "Transmission properties of composite metamaterials in free space", *Appl. Phys. Lett.* **81**, 120 (2002); K. Aydin et al., "Experimental observation of true left-handed transmission peak in metamaterials", *Optics Letters* **29**, 2623 (2004).

[11] M. Notomi, "Negative refraction in photonic crystals", *Phys. Rev. B* **62**, 10696 (2000); E. Cubukcu et al., "Negative refraction by photonic crystals", *Nature* **423**, 604 (2003); and "Subwavelength resolution in 2d photonic crystal-based superlens", *Phys. Rev. Lett.* **91**, 207401 (2003); S. Foteinopoulou and C. M. Soukoulis, "Negative refraction and left-handed behavior in 2d photonic crystals", *Phys. Rev. B* **67**, 235107 (2003).

[12] J. B. Pendry, "A chiral route to negative refraction", *Science* **306**, 1353 (2004).

[13] S. O'Brien and J. B. Pendry, ' 'Photonic band gap effects and magnetic activity in dielectric composites", *J. Phys: Condens. Matt.* **14**, 4035 (2002); K. C. Huang, M. L. Povinelli and J. D. Joannopoulos, " Negative effective permeability in polaritonic photonic crystals", *Appl. Phys. Lett.* **85**, 543 (2004).

[14] V. A. Podolskiy, A. K. Sarychev, and V. M. Shalaev, "Plasmon modes in metal nanowires and left-handed materials", *J. Nonlin. Opt. Phys. Mater.* **11**, 6574 (2002).

[15] V. M. Shalaev, et al., "Negative index of refraction in optical metamaterials", *Opt. Lett.* **30**, 3356 (2005).

[16] W. J. Padilla, et al., "Electrically resonant terahertz metamaterials: Theoretical and experimental investigations", *Phys. Rev. B* **75**, 041102(R) (2007).

[17] D. R. Smith, S. Schultz, P. Markos and C. M. Soukoulis, "Determination of permittivity and permeability of metamaterials from scattering data", *Phys. Rev. B* **65**, 195104 (2002).

[18] R. Marques, F. Medina, and R. Rafii-El-Idrissi, "Role of bianisotropy in negative permeability and left-handed metamaterials", *Phys. Rev. B* **65**, 144440 (2002).

[19] T. Koschny, M. Kafesaki, E. N. Economou, and C. M. Soukoulis, "Effective medium theory of left-handed materials", *Phys. Rev. Lett.* **93**, 107402 (2004).

[20] N. Katsarakis, T. Koschny, M. Kafesaki, E. N. Economou, E. Ozbay and C. M. Soukoulis, "Left- and right-handed transmission peaks near the magnetic resonance frequency in composite metamaterials", *Phys. Rev. B.* **70**, 201101(R) (2004).

[21] M. Kafesaki, Th. Koschny, J. Zhou, N. Katsarakis, I. Tsiapa, E. N. Economou and C. M. Soukoulis, "Electromagnetic behavior of left-handed materials", *Physica B* **394**, 148 (2007).

[22] N. Katsarakis, T. Koschny, M. Kafesaki, E. N. Economou and C. M. Soukoulis, "Electric coupling to the magnetic resonance of split ring resonators", *Appl. Phys. Lett.* **84**, 2943 (2004).

[23] M. Kafesaki, Th. Koschny, R. S. Penciu, T. F. Gundogdu, E. N. Economou and C. M. Soukoulis, "Left-handed metamaterials: detailed numerical studies of the transmission properties", *J. Opt. A: Pure Appl. Opt.* **7**, S12 (2005).

[24] P. Gay-Balmaz and O. J. F. Martin, "Electromagnetic resonances in individual and coupled split-ring resonators", *J. Appl. Phys.* **92**, 2929 (2002).

[25] N. Katsarakis, et al., "Magnetic response of split-ring resonators in the far infrared frequency regime", *Opt. Lett.* **30**, 1348 (2005).

[26] S. Linden et al., "Magnetic Response of Metamaterials at 100 THz", *Science* **306**, 1351 (2004).

[27] C. Enkrich et al., "Magnetic metamaterials at telecommunication and visible frequencies", *Phys. Rev. Lett.* **95**, 203901 (2005).

[28] P. Gay-Balmaz and O. J. F. Martin, "Efficient isotropic magnetic resonators", *Appl. Phys. Lett.* **81**, 939 (2002).

[29] J.D.Baena, L.Jelinek, R.Marqus, J.Zehentner, "Electrically small isotropic three-dimensional magnetic resonators for metamaterial design", *Appl. Phys. Lett.* **88**, 134108 (2006).

[30] I. Bulu, H. Caglayan, and E. Ozbay, "Experimental demonstration of labyrinth-based left-handed metamaterials", *Opt. Expr.* **13**, 10238 (2005).

[31] Th. Koschny, L. Zhang and C. M. Soukoulis, "Isotropic 3d left-handed and related metamaterials of the split-ring resonator and wire type", *Phys. Rev. B* **71**, 036617 (2005).

[32] K. Aydin, I. Bulu, K. Guven, M. Kafesaki, C. M. Soukoulis, and E. Ozbay, "Investigation of magnetic resonances for different split-ring resonator parameters and designs", *New Journal of Physics* **7**, 168 (2005).

[33] N. Katsarakis, M. Kafesaki, I. Tsiapa, E. N. Economou and C. M. Soukoulis, "High transmittance left-handed materials involving symmetric split-ring resonators," *Photonics and Nanostructures* **5**, 149 (2007).

[34] Th. Koschny, R. Moussa and C. M. Soukoulis, "Limits on the amplification of evanescent waves in left-handed materials", *J. Opt. Soc. Am. B* **23**, 485 (2006).

[35] D. R. Smith, D. C. Vier, Th. Koschny, and C. M. Soukoulis, "Electromagnetic parameter retrieval from inhomogeneous metamaterials", *Phys. Rev. E* **71**, 121103 (2005).

[36] T. Koschny, P. Markoš, D. R. Smith, and C. M. Soukoulis, "Resonant and anti-resonant frequency dependence of the effective parameters of metamaterials", *Phys. Rev. E* **68**, 065602 (2003).

[37] Th. Koschny, P. Markoš, E. N. Economou, D. R. Smith, D. C. Vier, and C. M. Soukoulis, "Impact of inherent periodic structure on effective medium description of left-handed and related metamaterials", *Phys. Rev. B* **71**, 245105 (2005).

[38] For recent reviews on optical NIMs see: V. M. Shalaev, "Optical negative-index materials", *Nature Photonics* **1**, 41 (2007); C. M. Soukoulis, S. Linden & M. Wegener, "Negative index metamaterials at optical wavelengths", *Science* **315**, 47 (2007); S. Linden et al., "Photonic metamaterials: Magnetism at optical frequencies",

*IEEE J. of Selected Topics in Quant. Electr.* **12**, 1097 (2006).

[39] J. Zhou, Th. Koschny, M. Kafesaki, E. N. Economou, J. B. Pendry & C. M. Soukoulis, "Saturation of the magnetic response of split-ring resonators at optical frequencies", *Phys. Rev. Lett.* **95**, 223902 (2006).

[40] C. M. Soukoulis, Th. Koschny, J. Zhou, M. Kafesaki, E. N. Economou, "Magnetic response of split-ring resonators at terahertz frequencies", *Phys. Stat. Sol. (b)* **244**, 1181 (2007).

[41] L. Solymar, *Lectures on Electromagnetic Theory* (Oxford University Press, Oxford, 1976).

[42] S. Tretyakov, "On geometrical scaling of split-ring and double-bar resonators at optical frequencies", *Metamaterials* **1**, 40 (2007).

[43] M. W. Klein, C. Enkrich, M. Wegener, C. M. Soukoulis, & S. Linden, "Single-slit split-ring resonators at optical frequencies: Limits of size scaling", *Opt. Lett.* **31**, 1259 (2006).

[44] J. Zhou, E. N. Economou, Th. Koschny & C. M. Soukoulis, "A unifying approach to left handed materials design", *Opt. Lett.* **31**, 3620 (2006).

[45] J. Zhou et al., "Negative index materials using simple short wire pairs", *Phys. Rev. B* **73**, 041101 (2006).

[46] J. Zhou et al., "'Experimental demonstration of negative of index of refraction", *Appl. Phys. Lett.* **88**, 221103 (2006).

[47] K. Guven, et. al., "Bilayer metamaterial: analysis of left-handed transmission and retrieval of effective medium parameters", *J. Opt. A: Pure Appl. Opt.* **9**, S361 (2007).

[48] . T. F. Gundogdu, et al., "Negative index short-slab pair and continuous wires metamaterials in the far infrared regime", *Opt. Expr.*, to appear.

[49] . M. Kafesaki, I. Tsiapa, N. Katsarakis, Th. Koschny, C. M. Soukoulis and E. N. Economou, "Left-handed metamaterials: The fishnet structure and its variations", *Phys. Rev. B* **75**, 235114 (2007).

[50] . S. Zhang, et al., "Experimental demonstration of near-infrared negative-index metamaterials", *Phys. Rev. Lett.* **95**, 137404 (2005); S. Zhang, et al., "Mid-infrared resonant magnetic nanostructures exhibiting a negativity permeability", *Phys. Rev. Lett.* **94**, 37402 (2005).

[51] R. Ulrich, "Far infrared properties of metallic mesh and its complementary structure", *Infrared Phys.* **7**, 37 (1967).

[52] G. Dolling, C. Enkrich, M. Wegener, C. M. Soukoulis and S. Linden, "A low-loss negative index metamaterial at telecommunication wavelengths", *Opt. Lett.* **31**, 1800 (2006).

[53] U. K. Chettiar et al., "Dual-band negative index metamaterials: Double-negative at 813 nm and single negative at 772 nm", *Opt. Lett.* **32**, 1671 (2007).

[54] N. Katsarakis et al., "Optimized left-handed behavior in microwaves, employing the fishnet design", *in preparation.*

[55] K. B. Alici, and E. Ozbay, "A planar metamaterial: Polarization independent fishnet structure", *Photonics and Nanostructures* **6**, 102 (2008).

[56] R. S. Penciu, et. al., "Slab-pairs and fishnet design: limits of size scaling", *in preparation.*

[57] G. Dolling, M. Wegener, C. M. Soukoulis and S. Linden, "Design-related losses of of double-fishnet negative-index photonic metamaterials", *Optics Express* **15**, 1153 (2007).

[58] A. K. Popov, and V. M. Shalaev, "Compensating losses in negative-index metamaterials with optical parametric amplification", *Opt. Lett.* **31**, 2169 (2006).